Model of linewidth for laser writing on a photoresist

José Ramón Salgueiro, Vicente Moreno, and Jesús Liñares

We present a theoretical model to describe the feature size produced by direct laser writing upon a photoresist relative to various experimental parameters. The model allows the number of parameters required for describing the linewidth to be reduced and shows how the description can be made in terms of the ratio of laser power to writing velocity. Both of the limiting cases of the truncation of the laser beam are analyzed; i.e., the case of a nontruncated (Gaussian) beam and the case of a strongly truncated beam (simplified with uniform illumination assumed). Experimental measurements are presented that are fitted to the model to permit its validity to be assessed and for a comparison of these two regimes, which are shown to be different.

OCIS codes: 350.3390, 110.5220.

1. Introduction

The technique of laser writing is appreciated by researchers because of its broad field of applications to surface science and material processing (annealing, deposition, micromachining, etc.).[1–3] It consists of using a focused laser beam to process a material that is moved by means of a motorized stage under the laser spot. This technique also constitutes a powerful tool for fabricating optical devices, particularly for fabrication of masks, when the substrate is coated with a photoresist film such that a laser spot makes an exposure to draw a pattern that is then transferred to the photoresist. Some of its well-known characteristics, which make it so attractive, are low cost, technical simplicity, and good quality of the structures patterned, which exhibit smooth borders. This is why the literature describes the use of laser systems for many different purposes, such as obtaining masks for fabricating integrated devices,[4–7] fabricating micro-optic and diffractive elements,[8,9] and generating holograms.[10] The range of feature sizes that can be obtained is ~1 μm though submicrometer resolutions have been reported.[11–13] For all these reasons it is believed that laser writing in the future will compete with *e*-beam lithography for applications in mask fabrication and direct writing.[12,13]

To make the system useful requires previous characterization to allow the linewidths that correspond to various values of the experimental parameters to be obtained. The measured linewidth is usually plotted relative to a variable such as laser power or stage velocity such that one can keep track of the resultant linewidth when some particular experimental parameters are set and afterward program such parameters to obtain the desired structures. A theoretical model can be useful in two ways. First, it permits extrapolations of the characterization curves. Second, if some experimental conditions, such as photoresist type, photoresist processing conditions, laser wavelength, and focusing optics, are changed, it will not be necessary to repeat the whole characterization procedure; measurement of the linewidth for a small set of parameter values will be enough to produce the new linewidth curves. In this way one can quickly tune the system without the tedious task of repeated characterization.

In what follows, we present such a model. After a brief review of the spot profiles and sizes obtained from focusing a laser beam (Section 2) and of the behavior of a photoresist when it is exposed to light (Section 3), a model with which to describe the linewidth is developed in Section 4. Finally, in Section 5 we present experimental results and discussions of the model's performance.

The authors are with the Departamento de Física Aplicada, Universidade de Santiago de Compostela, Escola Universitaria de Óptica, Campus Sur, E-15782 Santiago de Compostela, Spain. J. R. Salgueiro's e-mail address is fajose@usc.es. Fax number: +34 981 590485.

Received 14 March 2001; revised manuscript received 27 September 2001.

0003-6935/02/050895-07$15.00/0

2. Laser Pencil's Shape and Size

To predict the effects of a focused beam on the substrate it is necessary to know the irradiance distribution that will account for the light transferred at each point on the substrate's surface. The spot shape depends basically on the light source and the focusing optics. The source is usually a laser beam with a Gaussian irradiance profile given by[14] $I(\rho) = 2P/(\pi w^2) \exp(-2\rho^2/w^2)$, where ρ is the radial cylindrical coordinate in the plane perpendicular to beam axis $\rho = (x^2 + y^2)^{1/2}$, P is the total power of the beam, and w is the beam radius, which has a convergent or divergent shape from its waist where it reaches its minimum width $2w_0$. The focusing optics is usually an objective, which forms a reduced image of the beam waist upon the substrate's surface. We restrict our discussion to the case of an aberration-free objective (for example, a microscope objective illuminated by a visible laser source). The objective's performance is usually described by its focal length f and by its numerical aperture NA, which constitutes a measure of the emergent ray cone amplitude in the image space and is directly related to aperture radius a, which can be expressed in terms of both f and NA (specifications by the objective's manufacturer) as $a = f\text{NA}$.[15]

If we assume that the objective is diffraction limited, the spot size and its profile will depend on how much the laser beam is limited by the aperture. In this way, we define the truncation relation by

$$\gamma = \frac{w}{a} = \frac{w}{f\text{NA}}. \tag{1}$$

The study of the shape and size of the laser spot is carried out by means of the diffraction theory. In Fig. 1 various spot irradiance profiles for different values of the truncation relation are shown. The curves in the figure, obtained by numerical evaluation of Kirchhoff's diffraction integral,[16] were obtained for a fixed aperture radius of $a = 2.5$ mm, which corresponds to a conventional 60× objective ($f = 2.9$ mm; NA, 0.85), and the varying radius of a beam whose wavelength is set at $\lambda = 457.9$ nm (Ar^+ laser). Figure 1 allows one to see the transition between small ($\gamma \ll 1$) and large ($\gamma \gg 1$) truncation, with the result that in the large-truncation limit the smallest focal spot is obtained, although secondary diffraction rings appear and an important fraction of the beam power is wasted because the spot diminishes exponentially with the truncation relation as $P' = P[1 - \exp(-2/\gamma^2)]$. Thus, for a fixed objective lens, each regime is interesting, depending on whether the requirements for the particular application are maximum resolution (smallest spot size) or better management of the laser power. If the necessary spot size is fixed, however, the optimal characteristics of the objective together with the truncation relation can be found, so as to minimize the power requirements.[17]

Kirchhoff's diffraction integral for a circular aperture can be analytically solved in terms of a series of Bessel functions.[18] However, a simple solution exists for the two limiting cases mentioned above. For $\gamma \ll 1$ the aperture does not influence the laser beam, so we obtain another Gaussian beam but one whose waist is transformed according to the magnification of the objective. In this case the irradiance profile as well as the spot size, measured at the points where the irradiance falls to a fraction $1/e^2$ of the maximum value, is given by

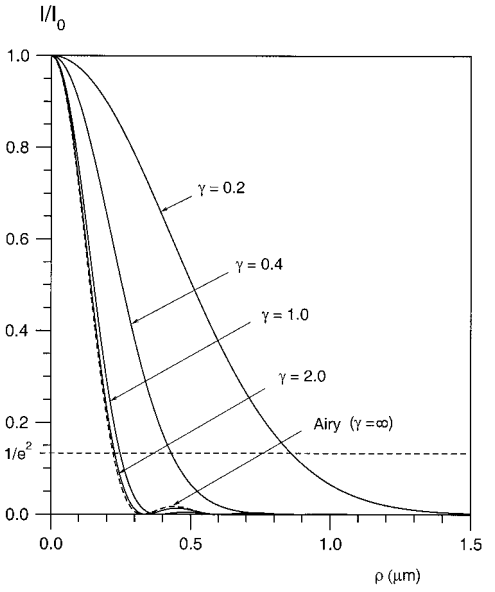

Fig. 1. Irradiance distribution of the focal spot for several values of truncation relation γ. The aperture radius is fixed at a value of $a = 2.5$ mm, corresponding to that for a conventional microscope 60× objective (=2.9 mm; NA, 0.85), and the laser beam radius was properly established for each curve to produce the truncation relation. Dashed curve, uniform illumination. The wavelength was set at 457.9 nm (Ar^+ laser).

$$I_g(\rho) = \frac{2P}{\pi w_g^2} \exp\left(-\frac{2\rho^2}{w_g^2}\right), \tag{2}$$

$$2w_g = \frac{4\lambda f}{\pi(2w)} = 1.27\frac{\lambda f}{2w}. \tag{3}$$

The subscript g has been used to label both magnitudes, denoting that they both correspond to the Gaussian case.

In the other limiting case, when the truncation relation is large ($\gamma \gg 1$), we have to consider only a small fraction of the beam close to the propagation axis. In this case the Gaussian nature of the beam is neglected, and the illumination can be considered uniform, yielding the well-known Airy diffraction pattern:

$$I_a(\rho) = \frac{P'\alpha^2}{4\pi}\left[\frac{2J_1(\alpha\rho)}{\alpha\rho}\right]^2, \tag{4}$$

$$\alpha = \frac{2\pi a}{\lambda f} = \frac{2\pi\text{NA}}{\lambda}, \tag{5}$$

$$2w_a = \frac{5.15}{\alpha} = 1.64\,\frac{\lambda f}{2a}. \tag{6}$$

Now the subscript a is used to indicate that the magnitudes correspond to the Airy profile. Besides the same criterion for determining the spot size as in the previous case has been considered (points where the irradiance falls to $1/e^2$ times the maximum value) rather than the usual criterion that takes into account the points at the first minimum of the diffraction pattern. In the latter case the spot size is given by $2w'_a = 2.44\lambda f/(2a)$, and the relation between the sizes obtained by the two criteria, is $w'_a = 0.67\, w_a$. Besides, the power is denoted P' to account for the fraction lost by the aperture truncation as cited above. The Airy profile [Eq. (4)] is also plotted in Fig. 1 (dashed curve) for comparison, with the result that a beam radius between once and twice the objective aperture radius often constitutes a good compromise between resolution and waste of power.

3. Photoresist Exposure

In most common light-sensitive photoresists, such as diazonaphthoquinone-novolak, the laser radiation during exposure induces photochemical modifications of a photoactive component that leads, during development, to an increase of photoresist dissolution rate in the developer. The result is the removal of more photoresist as the exposure dose increases, yielding a difference in the film thicknesses of the irradiated and the nonirradiated zones.

An elaborate model to describe the effects of radiation on photoresist was developed by Mack.[19] A parameter C, which is characteristic of the photoresist nature, wavelength of light and processing conditions, can be measured and used to describe the shape of the resulting structure. To evaluate easily the linewidth produced by writing with a laser spot, it is enough to consider the so-called dose-to-clear parameter ratio, D_0, related to parameter C and development conditions, which denotes the minimum exposure dose necessary to remove completely all the photoresist film in the irradiated region.[20] This parameter behaves consequently as an effective threshold dose, accounting for properties of the illumination source, the photoresist, and the substrate (reflectance) as well as for processing conditions. Hence one can determine the linewidth by locating the points that receive an exposure dose equal to D_0. Nevertheless, the resist contrast, which determines the border slope (region of partial exposure), can play an important role in determining what the effective value of the linewidth is, depending on the process that follows the resist development. For example, in reactive ion etching (RIE) the erosion of the photoresist influences the border of the etched material.[21] At any rate, redefining parameter D_0 makes the following treatment fully applicable.

Coating and development conditions are not considered here; we relate the following discussion only in terms of parameter D_0, which will account for whatever the fixed conditions are.

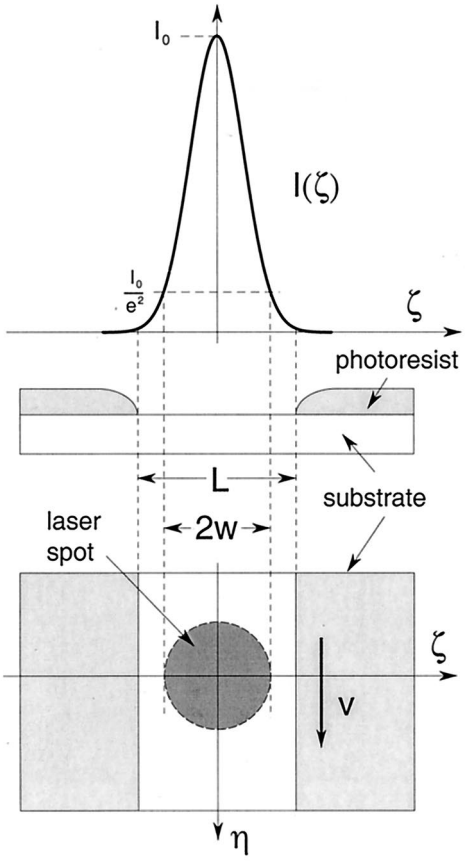

Fig. 2. Schematic of the laser spot profile (Gaussian profile) and the line drawn on the photoresist film, together with the reference system used.

4. Linewidth Model

To estimate the width of the line traced in the writing process, we should evaluate the amount of exposure transferred to the photoresist at each point under the laser spot and calculate at which points from its center this exposure dose equals the value of the dose-to-clear D_0. As this value D_0 establishes the minimum dose that will completely remove the photoresist film, linewidth L is the distance between these two points, as shown in Fig. 2. The value of D_0, as well as the irradiance profile and the beam power, determines whether the linewidth is larger or shorter than the spot size.

We define two mutually orthogonal coordinate axes in the substrate plane. Axis η is the direction of writing movement, and axis ζ is the direction normal to writing displacement. The polar coordinate is $\rho^2 = \eta^2 + \zeta^2$. We assume that the writing movement occurs at a constant velocity v. We determine the differential contribution of each spot point to the exposure dose on a particular surface substrate position by multiplying irradiance $I(\rho)$ by exposure time dt: $dD = I(\rho)/dt$, so we find the total exposure by adding all these differential contributions:

$$D(\zeta) = \int_{-\infty}^{+\infty} I(\rho)\,dt = \frac{2}{v}\int_{0}^{+\infty} I(\sqrt{\eta^2 + \zeta^2})\,d\eta, \qquad (7)$$

where the definition of velocity $v = d\eta/dt$ has been used. The line limits are given by point ζ_0 at which $D(\zeta_0) = D_0$, which in this case is linewidth $L = 2\zeta_0$, because we consider the spot to be circularly symmetric. Now we shall evaluate this linewidth for the two previously discussed extreme cases of irradiation: with a Gaussian nontruncated beam and with a uniform (highly truncated) beam.

A. Nontruncated Beam

For a nontruncated beam, using Eq. (2) in Eq. (7) yields the following exposure dose:

$$D_g(\zeta) = \frac{4P}{\pi v w_g^2}\exp\left(-\frac{2\zeta^2}{w_g^2}\right)\int_0^{+\infty}\exp\left(-\frac{2\eta^2}{w_g^2}\right)d\eta = \sqrt{\frac{2}{\pi}}\frac{P}{w_g v}\exp\left(-\frac{2\zeta^2}{w_g^2}\right). \quad (8)$$

Now, establishing the condition for line border $D_g(\zeta_0) = D_0$, we obtain

$$L_g = 2\zeta_0 = w_g\left[2\log\left(\sqrt{\frac{2}{\pi}}\frac{P}{D_0 w_g v}\right)\right]^{1/2}. \quad (9)$$

The first conclusion that we can draw is that the spot size constitutes the parameter that most influences linewidth. In fact, the other parameters, beam power and writing velocity, are under a logarithmic function, and this logarithm is under a square root, leading to a much steadier variation of the linewidth. The dependence of linewidth on power, velocity, and the photoresist dose-to-clear parameter, however, exhibits the same relative behavior, so the linewidth can be described by only one parameter, which accounts for the influence of the other three. We distinguish two kinds of parameters: those that are usually fixed, such as spot size and the exposure dose-to-clear, and those that are varied in real time to draw different-sized structures, such as laser power and stage velocity. According to these considerations we define

$$\Omega = \frac{P}{v}, \quad (10)$$

$$\kappa_g = \sqrt{\frac{2}{\pi}}\frac{1}{w_g D_0}, \quad (11)$$

so the linewidth can be written as

$$L_g = w_g[2\log(\kappa_g\Omega)]^{1/2}. \quad (12)$$

In this way, κ_g accounts for the fixed parameters and Ω for the variable ones. From the above expressions (10) to (12) we can see that, for a physically consistent result, it is necessary that $\Omega \geq \kappa_g$. This means that the laser power has to be high enough in relation to velocity and the dose-to-clear parameter to produce a sufficient dose of radiation to write a line. For lower values of Ω, the dose does not suffice to remove completely all the photoresist in any region under the laser spot.

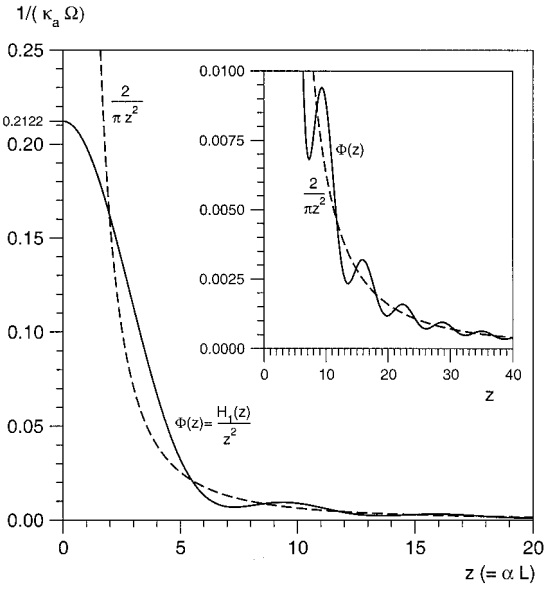

Fig. 3. Plot of $\Phi(z) = H_1(z)/z^2$ function (continuous curve) together with that which describes its asymptotic behavior, $2/(\pi z^2)$ (dashed curve). Inset, the region containing the secondary maxima plotted on a different scale for clarity.

B. Uniform Illumination

In case of uniform illumination, achieved when the laser beam is highly truncated by the objective aperture ($\gamma \gg 1$), we substitute the Airy irradiance distribution [Eq. (4)] into Eq. (7) to obtain

$$D_a(\zeta) = \frac{2P'\alpha^2}{\pi v}\int_0^{+\infty}\frac{J_1^2(\alpha\sqrt{\eta^2+\zeta^2})}{\alpha^2(\eta^2+\zeta^2)}d\eta. \quad (13)$$

The integration can be carried out by use of the following general formula[22]:

$$\int_0^{+\infty}\frac{J_\nu^2(\sqrt{t^2+z^2})}{(t^2+z^2)^\nu}t^{2\nu-2}dt = \frac{\Gamma[\nu-(1/2)]}{2z^{\nu+1}\sqrt{\pi}}H_\nu(2z), \quad (14)$$

where $H_\nu(z)$ is the Struve function of order ν. In this way we obtain

$$D_a(\zeta) = \frac{4\alpha P'}{\pi v}\Phi(2\alpha\zeta), \quad (15)$$

where the function $\Phi(z) = H_1(z)/z^2$ has been defined. This function, plotted in Fig. 3 (continuous curve), presents a principal maximum and secondary maxima produced because of the diffraction rings in the Airy pattern. However, the dose at the minima of $\Phi(z)$ is not zero, owing to the addition of all contributions of the spot profile for all the values of η and ζ fixed. According to Eq. (15) and for $D_a(\zeta_0) = D_0$, the linewidth is given by

$$L_a = 2\zeta_0 = \frac{1}{\alpha}\Phi^{-1}\left(\frac{1}{\kappa_a\Omega}\right) = \frac{w_a}{2.57}\Phi^{-1}\left(\frac{1}{\kappa_a\Omega}\right), \quad (16)$$

where $\Phi^{-1}(z)$ is the inverse function of $\Phi(z)$ and Eq. (6) has been used. Parameter Ω is defined by Eq. (10), whereas now we define κ_a as

$$\kappa_a = \frac{4\alpha}{\pi D_0}[1 - \exp(-2/\gamma^2)] = \frac{3.28}{w_a D_0}[1 - \exp(-2/\gamma^2)], \quad (17)$$

where we have included the factor of power truncation to maintain the definition of Ω in terms of total beam power P.

C. Broad-Line Regime

From the curve of $\Phi(z)$ shown in Fig. 3, one can realize that its inverse, $\Phi^{-1}(z)$, takes more than a single value for some values of z. This occurs at high values of Ω, for which the argument of $\Phi^{-1}(z)$ in Eq. (16) is small. In fact, because of the particular irradiance profile of the Airy pattern, some secondary lines can be obtained if the experimental variables (described globally by Ω) are properly set. The scale factor in the linewidth is given by the value of parameter α (inversely proportional to the spot size), as follows from Eq. (16), which can be also written in terms of the function $\Phi(z)$ as

$$\frac{1}{\kappa_a \Omega} = \Phi(\alpha L_a). \quad (18)$$

We can use Fig. 3 to obtain information about the theoretical behavior of the linewidth with respect to parameter Ω. In this way we can consider two different regimes. On the one hand, for low Ω, the linewidth is comparable with spot size w_a, and the point of the spot profile that corresponds to exposure D_0 falls upon the principal maximum of the Airy pattern. In this case the secondary maxima have no influence, as they do not supply enough exposure to eliminate the photoresist completely. On the other hand, for large values of Ω this threshold point falls upon the Airy pattern's wings. This means that for some values of Ω we obtain more than one value for the linewidth; these values correspond to the border of each line traced by each secondary maximum. However, the differences in amplitude of those maxima are tiny. Even so, effects, such as scattering in the photoresist film and defocus of the laser spot, make this secondary structure blurred such that it is not transferred to the photoresist. Besides, the former effect is enhanced by reflections in the substrate surface and the latter is specially important for high-NA objectives because the depth of focus is of the same order as the thickness of the photoresist film. Therefore, if we wish to describe the behavior of the linewidth properly we should search for a function with the same behavior as $\Phi(z)$ but without the oscillating characteristic, i.e., a function representing an average of $\Phi(z)$ through a distance comparable with its period. To do this we can consider the asymptotic expansion of the Struve function for z large[22]: $H_1(z) \sim Y_1(z) + 2/\pi + O(z^{-2})$, where $Y_1(z)$ is a Bessel function of the second kind of order 1. Because the dominant term is $2/\pi$, the behavior of function $\Phi(z)$ when its argument is large is

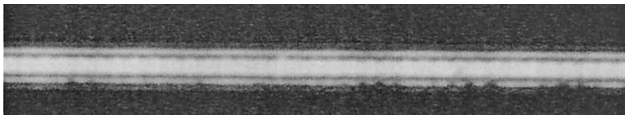

Fig. 4. Line traced with a 20× objective and Ω properly set to transfer the structure generated by the first secondary maximum of function Φ, patterned as an opening in a chromium mask by wet etching after development of the photoresist.

$$\Phi(z) \sim \frac{2}{\pi z^2}. \quad (19)$$

As this approximation is valid only for large values of z, the question arises: How large should z be such that $\Phi(z)$ can be properly described by approximation (19)? To answer this question we have plotted in Fig. 3 the function $\Phi(z)$ together with its asymptotic dominant behavior (dashed curve). We can establish that, for values of the argument larger than 7 or 8, approximation (19) constitutes a good description, and consequently it is valid when the linewidth is clearly greater than the spot size because, from Eq. (6), $z = \alpha L_a = 5.15 L_a/(2w_a)$; this is the broad-line regime. For values of the linewidth that are greater than the spot size the description is expected to be accurate, as the small difference in amplitude between high-order secondary maxima prevents the transference of this structure to the photoresist. For low-order maxima, however, if conditions are favorable (accurate focus positioning, high enough focal depth, etc.) it is possible to transfer this structure to the photoresist. For example, in Fig. 4 the structure from the first secondary maximum has been transferred to the photoresist film and to an underlying chromium film (after etching).

To obtain the functional form of the linewidth in this regime, we make use of Eq. (18) and approximation (19) to obtain

$$L_b = \left(\frac{2\kappa_a}{\pi \alpha^2}\Omega\right)^{1/2} = \kappa_b \sqrt{\Omega}, \quad (20)$$

where the subscript b indicates the broad-line regime. Parameter κ_b is defined as

$$\kappa_b = \frac{2}{\pi}\left\{\frac{2[1 - \exp(-2/\gamma^2)]}{\alpha D_0}\right\}^{1/2} = 0.56\left\{\frac{w_a[1 - \exp(-2/\gamma^2)]}{D_0}\right\}^{1/2}. \quad (21)$$

5. Experimental Study

Using an established laser writing system,[7] we have patterned lines under various experimental condi-

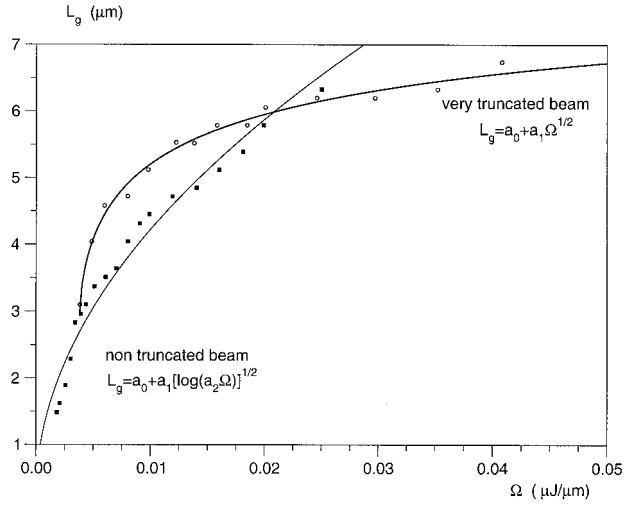

Fig. 5. Linewidth versus parameter Ω for the two limiting cases of a nontruncated ($\gamma \ll 1$) laser beam (Gaussian spot profile) and a strongly truncated ($\gamma \gg 1$) beam (uniform illumination), together with the respective fits to the corresponding theoretical functions. A 20× microscope objective (f = 8.3 mm; NA, 0.40) was used.

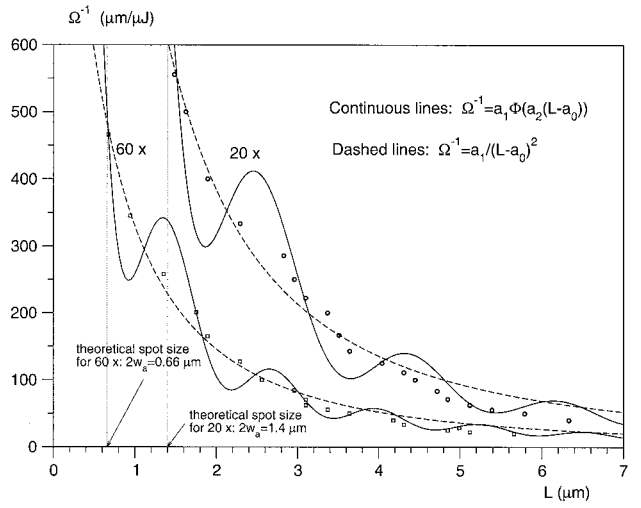

Fig. 6. Linewidth versus parameter Ω {in this case the inverse of parameter Ω^{-1} can perform the fit to function Φ: $\Omega^{-1} = a_1\Phi[a_2(L - a_0)]$} for two microscope objectives, 20× (f = 8.3 mm; NA, 0.40) and 60× (f = 2.9 mm; NA, 0.85). In addition to the fit to the Φ function the fit to its asymptotic form, $\Omega^{-1} = a_1/(L - a_0)^2$, is also plotted.

tions. The line λ = 457.9 nm from an Ar^+ laser is used as the light source, and an acousto-optic modulator establishes the beam power. The power is measured by a photometer, to which a beam split from the writing beam is directed. Thus the power measured may not necessarily be that of the writing beam but will anyway be proportional to it, and the study can be performed in terms of this measurement. The photometer is connected to a computer that controls the acousto-optic modulator by means of a general-purpose interface bus to provide feedback and better control of the power. The same computer also drives the stage controller to execute the writing movement. We prepared the substrates by spin coating microscope slides with Shipley S1813 photoresist to obtain a film that was ~1 μm thick. Coating conditions (spinning speed and time, postbake temperature and time, etc.) as well as developing conditions (developer concentration, time, temperature, etc.) were fixed and maintained such as not to influence the resultant linewidth (D_0 fixed). The parameters that we varied in the study were laser power and velocity. After processing the substrates, we measured the linewidth in each case by means of a microscope with a CCD attached to catch the image and get the linewidth in a simple processing task.

First, we made experiments for both strongly truncated and nontruncated beams to compare the two regimes. The results are plotted in Fig. 5. Data were fitted to the functions $L_a = a_0 + a_1[\log(a_2\Omega)]^{1/2}$ and $L_b = a_0 + a_1\sqrt{\Omega}$ for the Gaussian and the truncated cases, respectively. The fits seem to describe the experimental data fairly accurately and show that the two cases are qualitatively different, which justifies their separate treatment, and also indicate that the intermediate behavior between nontruncated and uniform illumination should be described by a function with an intermediate regime between $\sqrt{\Omega}$ and $\sqrt{\log \Omega}$. Parameters a_1 and a_2 are related to κ_g or κ_b through Eqs. (12) and (20) and allow the characteristic linewidth curves to be built. In both cases an additional parameter, a_0, was introduced to improve the fit, because the size of the linewidth is influenced by effects such as scattering of light inside the photoresist film and reflection on the substrate and by resist parameters such as finite thickness, contrast, and process bias. However, these effects also influence the other fitted parameters.

In the truncated case some undulating behavior of the experimental points about the curve is present because of the asymptotic approximation of function Φ (broad-line regime) for performing the fit. In fact, this secondary structure of function Φ is responsible for the deviations seen. This fact is better illustrated in Fig. 6, where the fit to function Φ [Eq. (18)] is presented. At some points the horizontal separation is larger and the slope seems to undergo a change produced by filling of the intermediate space between the principal line and the secondary line as a result of blurring. The effect is especially visible with the 20× objective and is not so evident with the 60× objective because of the larger focal depth in the first case, which results in less blurring and consequently in a greater influence of the secondary structure.

High truncation relation is usually more interesting because the power requirements for exposing the photoresist are not severe and then this regime permits higher resolution (a smaller spot). Besides, by setting Ω high enough it is also possible to draw much broader lines than the spot size, resulting in great flexibility of the writing process. Figure 7 shows a plot of the linewidth versus laser power for several values of the writing speed. The curves were traced with a 60× microscope objective (f = 2.9 mm; NA, 0.85) to produce

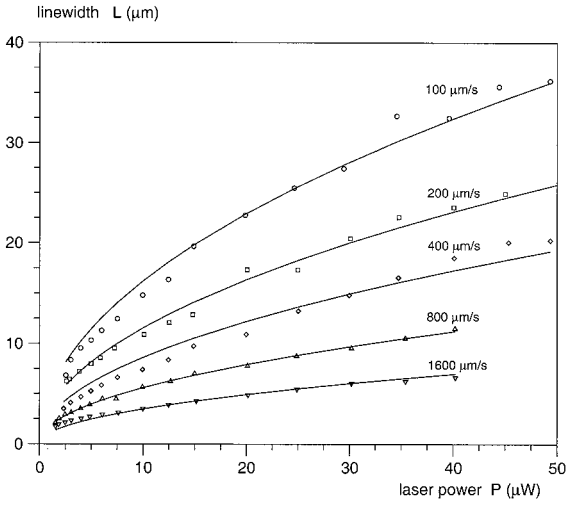

Fig. 7. Linewidth versus laser power for several values of writing speed and fits to the theoretical function in the broad-line regime.

Table 1. Parameters of the Fit of Linewidth Relative to Laser Power and Parameter κ_b

v (μm/s)	a_1 $\left(\frac{\mu m}{\mu W^{1/2}}\right)$	κ_b $\left(\frac{\mu m^{3/2}}{\mu J^{1/2}}\right)$
100	2.56	25.63
200	1.83	25.82
400	1.36	27.25
800	0.88	25.00
1600	0.55	21.98

a very small spot ($2w_a = 0.66$ μm). The experimental data were fitted to the function $L_b = a_1\sqrt{P}$, so parameter a_1 is directly related to $\kappa_b/\sqrt{v}$ through Eq. (20). In Table 1 we list the parameters obtained from the fit together with the values of κ_b obtained by taking the writing velocity into consideration in each case ($\kappa_b = a_1\sqrt{v}$). We can see that κ_b takes more-or less the same value for every speed, which confirms the dependence of linewidth on the ratio of laser power to writing velocity. In this case an additional parameter, a_0, can also be used in the fit to improve it and to account for the effects described above.

6. Conclusions

In this paper we have presented a simple model to describe the widths of the lines written on a photoresist as a function of various experimental parameters. Such a model has been found useful for calibrating and fast tuning such a system by making only a few measurements. The cases of no truncation (no wasted power) and strong truncation (minimum spot size) of the laser beam by the objective aperture were considered, and formulas to calculate the linewidth for each one were presented, demonstrating that both requirements are qualitatively different. In both cases the linewidth has been shown to depend on the ratio of beam power to writing velocity, which allows these two parameters to be reduced to only one. Finally, a fit of the experimental measurement to the theoretical model demonstrated that the theoretical expressions have provided a good description of the experimental data.

This study was supported by Xunta de Galicia, Spain, under contract PGIDTOOTIC20601PR.

References

1. D. Bäuerle, *Laser Processing and Chemistry*, 2nd ed. (Springer-Verlag, Berlin, 1996).
2. S. M. Metev and V. P. Veiko, *Laser-Assisted Micro-technology*, 2nd ed. (Springer-Verlag, Berlin, 1998).
3. H.-G. Rubahn, *Laser Applications in Surface Science and Technology* (Wiley, Chichester, UK, 1999).
4. K. E. Wilson, C. T. Mueller, and E. M. Garmire, "Laser writing of masks for integrated optical circuits," IEEE Trans. Components Hybrids Manuf. Technol. **CHMT-5,** 202–204 (1982).
5. M. Haruna, S. Yoshida, H. Toda, and H. Nishihara, "Laser-beam writing system for optical integrated circuits," Appl. Opt. **26,** 4587–4592 (1987).
6. M. G. Lad, G. M. Naik, and A. Selvarajan, "Laser patterning system for integrated optics and storage applications," Opt. Eng. **32,** 725–729 (1993).
7. J. R. Salgueiro, J. F. Román, and V. Moreno, "System for laser writing to lithograph masks for integrated optics," Opt. Eng. **37,** 1115–1123 (1998).
8. M. T. Gale, M. Rossi, J. Pedersen, and H. Shütz, "Fabrication of continuous-relief micro-optical elements by direct laser writing in photoresists," Opt. Eng. **33,** 3556–3566 (1994).
9. M. Haruna, M. Takahashi, K. Wakahayashi, and H. Nishihara, "Laser beam lithographed micro-Fresnel lenses," Appl. Opt. **29,** 5120–5126 (1990).
10. U. Krackhardt, J. Schwider, M. Schrader, and N. Streibl, "Synthetic holograms written by a laser pattern generator," Opt. Eng. **32,** 781–785 (1993).
11. H. Becker, R. Caspary, C. Toepfer, M. V. Schickfus, and S. Hunklinger, "Low-cost direct writing lithography system for the sub-micron range," J. Mod. Opt. **44,** 1715–1723 (1997).
12. P. C. Allen and P. Buck, "Resolution performance of a 0.60 NA, 364 nm laser direct writer," in *Optical/Laser Microlithography III*," V. Pol, ed., Proc. SPIE **1264,** 454–465 (1990).
13. W. Maurer, "Maskenschreiben mit Laser," Verein Deutcher Ingenieure (Springer-VDI-Verlag, Düsseldorf, Germany) Berichte **795,** 115–135 (1989).
14. B. E. A. Saleh and M. C. Teich, *Fundamentals of Photonics* (Wiley, New York, 1991).
15. M. Pluta, *Advanced Light Microscopy* (Polish Scientific, Warsaw, 1988), Vol. 1. Chap. 2.
16. J. J. Stamnes, *Waves in Focal Regions* (Hilger, Bristol, UK, 1986), Chap. 12.
17. H. M. Haskal, "Laser recording with truncated Gaussian beams," Appl. Opt. **18,** 2143–2146 (1979).
18. P. Kuttner, "Image quality of optical systems for truncated Gaussian laser beams," Opt. Eng. **25,** 180–183 (1986).
19. C. A. Mack, "Absorption and exposure in positive photoresist," Appl. Opt. **27,** 4913–4919 (1988).
20. R. Dammel, *Diazonaphthoquinone-Based Resists* (SPIE, Bellingham, Wash., 1993), Chap. 2.
21. W. M. Moreau, *Semiconductor Lithography. Principles, Practices, and Materials* (Plenum, New York, 1988), Chap. 13.
22. G. N. Watson, *A Treatise on the Theory of Bessel Functions* (Cambridge U. Press, Cambridge, UK 1966), Chap. 13.